

# Wireless crack sensing using an RFID-based folded patch antenna

Xiaohua Yi, Yang Wang, Roberto T. Leon

*School of Civil and Environmental Engineering, Georgia Institute of Technology, Atlanta, GA 30332, USA*

James Cooper, Manos M. Tentzeris

*School of Electrical and Computer Engineering, Georgia Institute of Technology, Atlanta, GA 30332, USA*

**ABSTRACT:** This paper describes the crack sensing performance of a wireless and passive smart-skin sensor designed as a folded patch antenna. When strain/deformation occurs on the patch antenna, the antenna's electrical length changes and its electromagnetic resonance frequency also changes accordingly. An inexpensive off-the-shelf radiofrequency identification (RFID) chip is adopted in the sensor design for signal modulation and collision avoidance. With assistance from the RFID chip, the resonance frequency change can be interrogated and recorded by a wireless reader. The RF interrogation energy from the reader is captured by the patch antenna, and then used to activate the RFID chip that transmits modulated signal back to the reader. Therefore, the interrogation process is wireless and the antenna sensor is battery-free. In this research, crack sensing performance of the antenna sensor is studied and tested by a specially designed crack testing device. Testing results show strong correlation between interrogated resonance frequency and crack opening size.

## 1 INTRODUCTION

Engineering structures, including those made of metallic materials, are susceptible to deterioration and damage due to cyclic loading and corrosive environment over their service lives. For example, fatigue-induced fracture/crack in steel bridges is of particular concern for inspectors and owners (ASCE 2009). Early detection of cracks is important for preventing catastrophic failures and prolonging a structure's service life (Dasgupta and Pecht 1991; Stephens *et al.* 2000). Current biennial bridge inspection mandated by the Federal Highway Administration is primarily visual (AASHTO 2009). Visual inspection is not effective for identifying cracks at locations difficult to access, or small-size cracks hidden under paint.

To address these difficulties, various nondestructive evaluation (NDE) techniques have been developed for crack detection in the last several decades (ASNT 2009). Different types of sensors and sensing systems have been investigated, such as piezoelectric sensors/actuators (Ihn and Chang 2004), acoustic emission systems (Roberts and Talebzadeh 2003), piezoelectric wafer active sensor (Giurgiutiu 2005), etc. However, most current sensing systems can be expensive or labor-intensive to deploy. The operation may be time-consuming or demand significant amount of electric power. These limitations make existing technologies impractical for large-scale/large-area deployment and continuous moni-

toring in the field.

In recent years, there has been interest in exploiting radiofrequency (RF) techniques for wireless strain sensing and crack detection. The basic sensing mechanism is enabled by the change in an antenna's electrical length when strain or crack occurs in the antenna (usually with 2D shape). As a result of the electrical length change, electromagnetic resonance frequency of the antenna also changes (Balanis 1997). By measuring the resonance frequency shift, deformation experienced by the antenna may be derived. For example, a patch antenna sensor is designed for crack testing by Deshmukh *et al.* (2010); this device requires light-switched circuitry for electromagnetic signal modulation by the sensor.

This research adopts the radio frequency identification (RFID) technology for signal modulation in an antenna sensor. RFID technology provides a means of wirelessly transferring data between a reader and a nearby RFID tag, which is usually attached to an object that is being identified and tracked (Finkenzeller 2003). The technology has numerous industrial applications, such as access management, toll collection, retail tracking, etc. In our previous study, a folded patch antenna was developed as a passive wireless strain sensor for metallic structures (Yi *et al.* 2011a). The sensor operation utilizes a backscattering mechanism, which refers to the deflection of electromagnetic wave from an object back to the source. A low-cost off-the-shelf RFID chip is adopted to make the sensor passive,

i.e., the sensor obtains all its operation power from the interrogation RF signal emitted by a wireless reader. Thus, the need for a battery or wired power source is eliminated. The sensing resolution and measurement limit of the RFID antenna sensor were investigated through extensive tensile tests (Yi *et al.* 2011b). It was shown that the prototype passive wireless strain sensor can detect small strain changes ( $<20 \mu\epsilon$ ), and perform well at large strains ( $> 10,000 \mu\epsilon$ ).

In this research, crack sensing performance of the prototype antenna sensor is investigated. Numerical simulations of crack sensing are first performed using a commercially available electromagnetic software package. To verify the crack sensing performance, a crack testing device is designed and fabricated. The antenna sensor is installed on the device, where a crack opening with growing sizes is generated. The antenna resonance frequency changes are measured and the results show an approximately linear relationship between the resonance frequency and the crack opening size. The paper is organized as follows. Section 2 introduces the crack sensing mechanism and the wireless interrogation mechanism for the antenna sensor. The crack simulation results for the antenna sensor are also presented. Section 3 provides experimental results illustrating the crack sensing performance of the antenna sensor. Finally, Section 4 provides a summary and discussion of this work.

## 2 WIRELESS INTERROGATION AND SENSOR DESIGN

The RFID wireless interrogation system usually consists of two components, an RFID reader and an RFID tag, as shown in Fig. 1. The RFID reader, which includes a reader unit and a reader antenna, serves for two functions, i.e. emitting interrogation RF signal and receiving modulated signal reflected from the tag. In general, the interrogation signal emitted by the reader is reflected back by both the RFID tag and other objects in the surrounding environment. For the reader to distinguish which part of the reflection is from the tag, signal modulation needs to be performed at the tag side.

The RFID tag includes an electromagnetic antenna and an RFID chip. The tag antenna receives interrogation signal from the reader and the RFID chip harnesses operational energy from the signal. By switching on/off an electrical load, the RFID chip transmits amplitude-modulated signal back to the reader. The reader finally demodulates the reflected signal, so that reflection by the tag can be differentiated from reflection by any other objects in the surrounding environment.

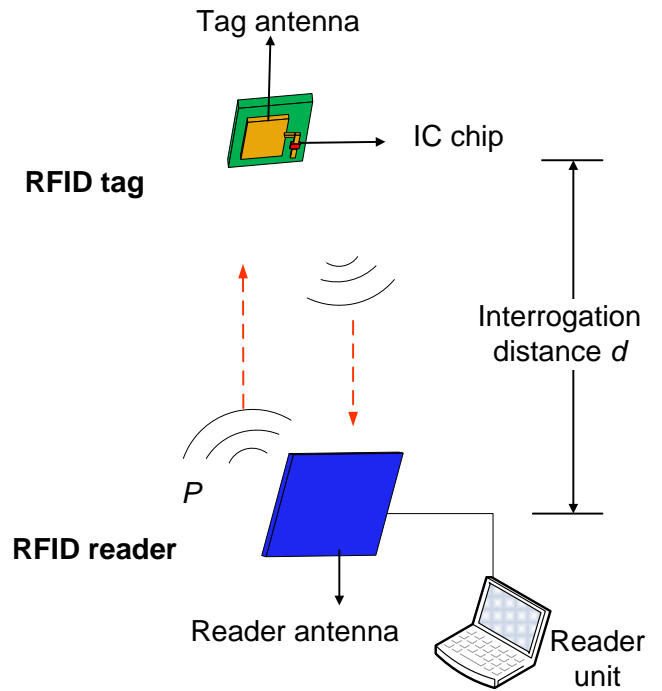


Fig. 1. Power transmission and backscattering in a passive RFID tag-reader system for wireless strain sensing

### 2.1 Sensor design

A folded patch antenna, as part of the RFID tag, is designed to function as a wireless strain sensor (Yi *et al.* 2011a). Fig. 2 shows the design drawing and a photo of the manufactured tag. To provide good radiation performance on metallic structures, a patch form is adopted for the antenna. Furthermore, the patch antenna is folded to reduce overall footprint. Vias are used to connect the top copper layer with bottom copper layer (i.e. ground plane) to achieve the “folding”. The substrate sandwiched between the top and bottom copper layers is made of Rogers RT/duroid<sup>®</sup>5880 material, a glass microfiber reinforced poly-tetra-fluoro-ethylene (PTFE) composite. The substrate thickness is 31 mils. The adopted RFID chip is the SL3ICS1002 model from NXP Semiconductors. Excluding soldering pads, physical size of the RFID chip is about  $1\text{mm}\times 1\text{mm}$ , as shown in Fig. 2(b). The chip impedance is  $13.3-j122 \Omega$  (“ $j$ ” is the imaginary unit) at 915 MHz, which is low and relatively easy to match during the tag antenna design. Meanwhile, impedance of the tag antenna can be tuned by adjusting the dimensions of the antenna design. When the impedance of the RFID chip equals the complex conjugate of the antenna impedance, the tag is matched and reaches its resonance frequency. The resonance frequency,  $f_{R0}$ , of the antenna can be estimated as:

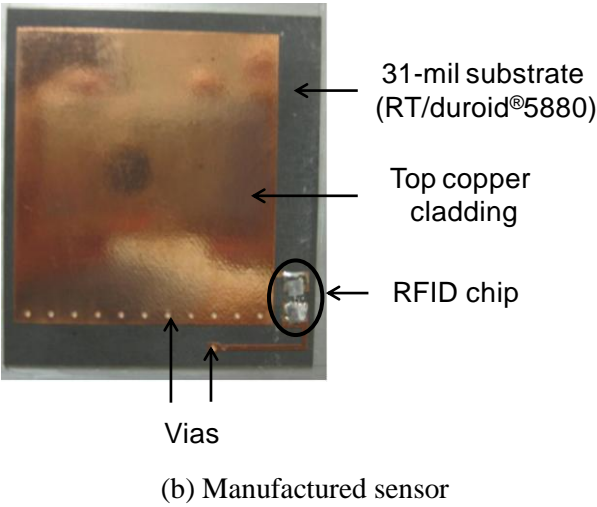
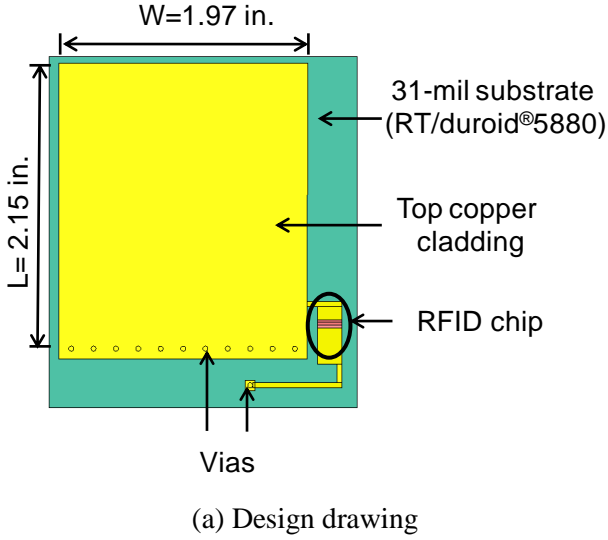


Fig. 2. RFID tag as an antenna sensor

$$f_{R0} = \frac{c}{4(L+L')\sqrt{\epsilon_r}} \quad (1)$$

where  $c$  is the speed of light,  $L$  is the electrical length of the antenna,  $L'$  is additional length compensation due to fringing effect, and  $\epsilon_r$  is the dielectric constant of the substrate. The electrical length of the sensor, for the original design, is equivalent to the physical length of the top copper layer.

## 2.2 Wireless interrogation mechanism

During interrogation, the RFID reader searches through a pre-specified frequency range to identify the resonance frequency of the tag. At certain interrogation frequency, the least amount of reader interrogation power required to activate the RFID chip is labeled as the interrogation power threshold. Fig. 3 illustrates the relationship between the interrogation power threshold for an antenna sensor and the interrogation frequency. For the case with no crack, when reader interrogation frequency equals the resonance frequency of an antenna sensor,  $f_{R0}$ , the interrogation power threshold reaches its minimum val-

ue. After a crack occurs along the ground plane or top copper layer of an antenna sensor, the resonance frequency shifts down to  $f_R$ . Thus the interrogation power threshold reaches its minimum value at  $f_R$ . This phenomenon can be explained by the electric current flow in the antenna. When the ground plane (or top copper layer) is cracked along the width direction of the antenna, current flow along the length direction is cut off and forced to detour along the crack. The elongated new electrical length decreases the resonance frequency of the sensor, as indicated by Eq. (1).

The RFID reader unit adopted in this application is the Tagformance Lite model made by Voyantic Ltd., which is capable of measuring interrogation power threshold. The reader sweeps through a predefined interrogation frequency range with a frequency resolution of 0.1 MHz. At every interrogation frequency, the reader searches at a power resolution of 0.1 dBm to identify the interrogation power threshold. Through a USB 2.0 port, a computer interface is used to operate and retrieve measurement data from the reader.

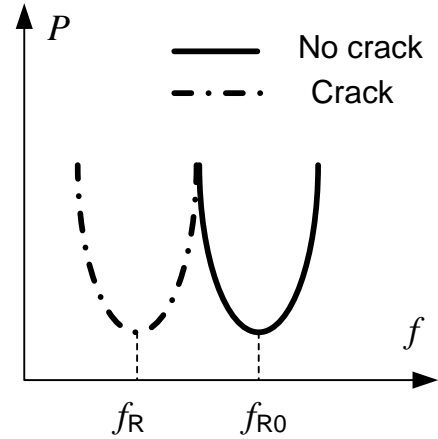


Fig. 3. Conceptual illustration of resonance frequency shift due to crack

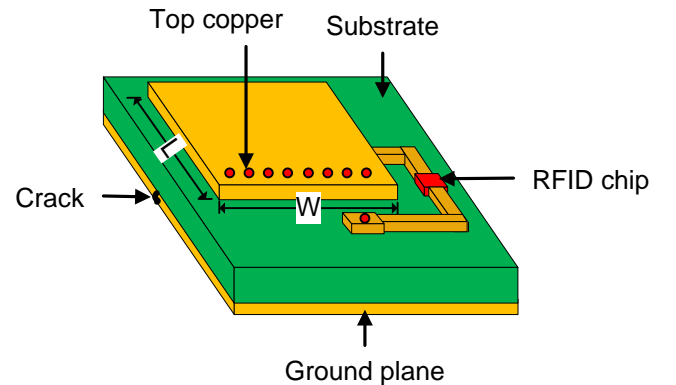


Fig. 4. Illustration of crack simulation model (not to scale)

### 2.3 Crack simulation

Numerical simulations are conducted using HFSS, a commercial electromagnetic software package, to study the effect of a crack on the resonance frequency shift of the antenna sensor. Fig. 4 shows the antenna sensor model being simulated. To transmit modulated signal through the tag antenna back to the reader, the RFID chip infuses RF power into the tag antenna. The majority part of the power leaves the antenna and gets transmitted into the air; yet unavoidably, a small fraction of the power is reflected by the tag antenna back to the chip. The power reflection coefficient,  $S_{11}$ , of the tag antenna quantifies this transmission efficiency.  $S_{11}$  is defined as the ratio of the power reflected by the tag antenna over the power infused by the RFID chip. A smaller value of  $S_{11}$  indicates higher transmission efficiency. In dB scale,  $S_{11}$  at frequency  $f$  can be calculated using the impedances of the RFID chip and the tag antenna (Kurokawa 1965):

$$S_{11}(f) = 10 \log \left| \frac{Z_{\text{Chip}}(f) - Z_{\text{Ant}}^*(f)}{Z_{\text{Chip}}(f) + Z_{\text{Ant}}(f)} \right|^2 \quad (2)$$

where  $Z_{\text{Chip}}$  and  $Z_{\text{Ant}}$  represent the impedance of the chip and the tag antenna, respectively. Both impedance parameters are usually functions of interrogation frequency  $f$  and superscript “\*” represents the conjugate of a complex number. Although the analytical form of  $S_{11}$  as a function of the interrogation frequency  $f$  is in general difficult to obtain,  $S_{11}(f)$  can be computed numerically. The  $S_{11}(f)$  plot reaches minimum value when the interrogation frequency  $f$  equals the resonance frequency of the tag antenna,  $f_{R0}$ . In other words, at resonance frequency  $f_{R0}$ , the highest transmission efficiency is achieved by the tag antenna.

The initial resonance frequency of the antenna sensor is studied by simulating the power reflection coefficient  $S_{11}$  at different frequencies. As illustrated in Fig. 5, the  $S_{11}(f)$  plot of the original antenna shows the initial resonance frequency to be 912.07 MHz. When a 200 mil  $\times$  4 mil crack is introduced along the width direction of the ground plane, i.e. bottom copper layer, the updated  $S_{11}(f)$  shows the resonance frequency changes to 907.1 MHz. In other words, a decrease in antenna resonance frequency is observed as the crack is introduced to ground plane.

### 3 EXPERIMENTAL RESULTS FOR CRACK SENSING

A crack testing device is designed for the experiments. As shown in Fig. 6, the crack testing device consists of three aluminum plates, i.e. a base plate (16in.  $\times$  12in.  $\times$  1in.), a top rotating plate (8in.  $\times$  4in.  $\times$  0.5in.), and a fixed bottom plate (8in.  $\times$  4in.  $\times$  0.5in.). The bottom plate is fastened to the base plate

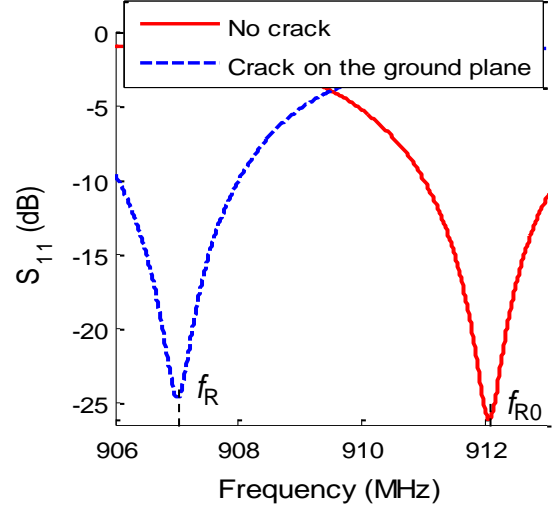


Fig. 5. Crack simulation results

by four corner bolts. The rotating plate is attached to the base plate by one bolt at a rotation axis at the bottom right and a fine-resolution displacement control screw (1/24 in. threading) at the top left. By turning the screw, a rotation is imposed on the top plate and a crack is opened between the top and bottom plates. The crack opening size is measured by a digital dial gage (0.0001 in. resolution) mounted at the left side of the base plate. A spring-loaded probe from the gage pushes against an angle bracket that is fastened to the left edge of the rotating plate.

For crack testing, the back side of a prototype antenna sensor is bonded with the rotating and fixed plates, above the gap. The experimental setup is shown in Fig. 7. The reader antenna faces the center of the prototype sensor at a distance of 12 in. Through a coaxial cable, the reader antenna is connected with the Tagformance Lite reader unit. At each crack opening size, the Tagformance reader sweeps through a frequency range to measure the interrogation power threshold, and thus, to determine

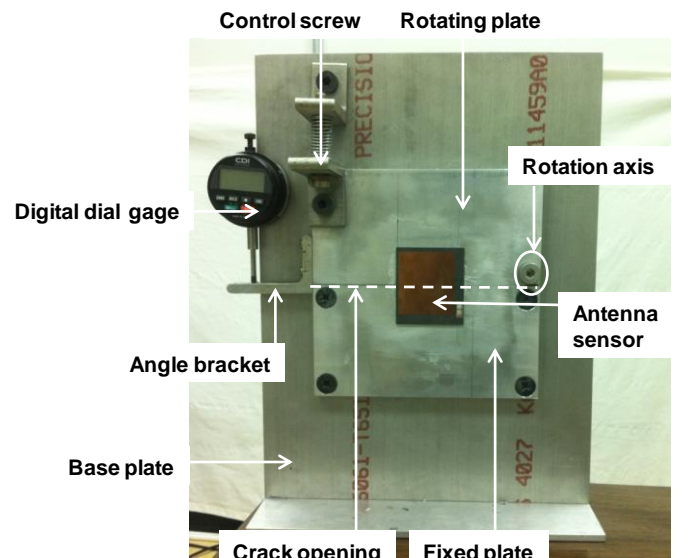


Fig. 6. Photo of the crack testing device

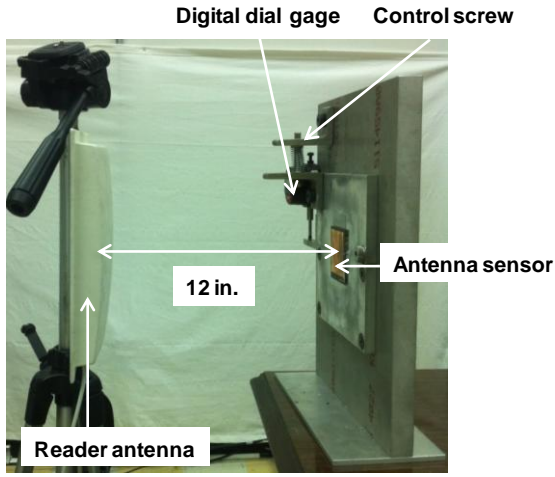


Fig. 7. Experimental setup

the resonance frequency of the antenna sensor. To reduce measurement noise, a total of five sweeps are conducted at each crack opening size. The average interrogation power threshold is calculated as:

$$\bar{P}(f) = \frac{1}{5} \sum_{i=1}^5 [P^i(f)] \quad (3)$$

where  $\bar{P}(f)$  is the average interrogation power threshold and  $P^i(f)$  is the interrogation power threshold from the  $i^{\text{th}}$  sweep. The units for the power parameters are dBm, measuring the power in decibels (dB) with respect to one milli-watt (mW). After the reader finishes interrogation at one crack opening size, the displacement control screw is turned to reach the next crack opening size.

A total of fourteen crack opening sizes were used during the experiment, before the antenna sensor stopped functioning properly at a 32-mil crack opening. For clarity, Fig. 8 shows the interrogation power threshold plots for only five crack opening sizes. The legend illustrates crack sizes estimated under-

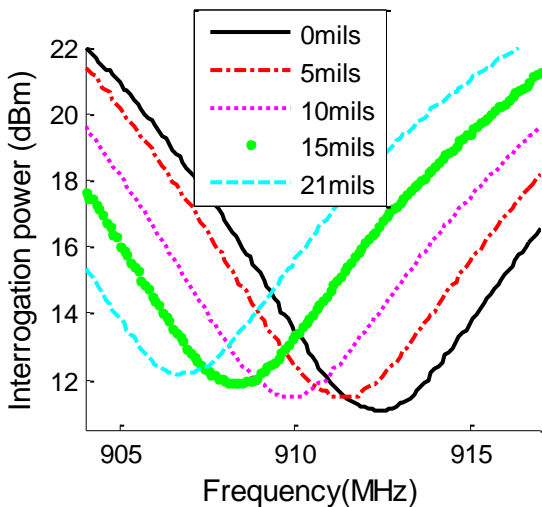


Fig. 8. Interrogation power threshold plots at different crack opening sizes

neath the sensor. The antenna resonance frequency is shown to reduce gradually when the size of the crack opening increases. Fig. 9 shows representative photos of the deformed/cracked antenna sensor at three different crack opening sizes. Fig. 9(a) shows the sensor at 5mils crack opening. No fracture occurs on the sensor, but slight deformation is observed on the top copper layer. Fig. 9(b) shows when crack opening is 21 mils, which is the last step presented in Fig. 8. Small fractures have developed on the top copper and the substrate, but the sensor still functions properly. Fig. 9(c) shows when a crack grows through the entire antenna width. At this point, no response from the antenna sensor can be received by the Tagformance reader.



(a) 5 mils



(b) 21 mils



(c) 32 mils

Fig. 9. Photos of deformed antenna sensor at different crack opening sizes

Since the valley areas of the resonance frequency plots in Fig. 8 are somewhat flat, the precise resonance frequency is not obvious in the plot. To resolve this difficulty, a 4<sup>th</sup> order polynomial curve fitting is performed to the valley area of each  $\bar{P}(f)$  plot. The value of the fitted 4th order polynomial is re-calculated at a frequency step of 0.001 MHz, in order to identify the resonance frequency that corresponds to the lowest interrogation power threshold.

The resonance frequency ( $f_R$ ) is plotted against each crack opening size ( $d$ ) in Fig. 10. A linear regression is performed on the fourteen data points. The slope of -0.3013 MHz/mil represents the crack sensing sensitivity, which means one mil crack underneath the sensor generates 0.3013 MHz decrease in resonance frequency. The initial resonance frequency at zero crack size is measured as 912.822 MHz, which is quite close to the simulation result (912.07 MHz). The coefficient of determination,  $R^2$ , is 0.9957 for the linear regression.

It should be noted that as shown in Fig. 9, physical phenomenon in the crack testing is a complicated process. At the beginning of the experiment, crack opening generated by the rotating plate causes stress concentration along the center line of the sensor ground plane, i.e. bottom copper layer. The strain/deformation also transfers into the substrate and the top copper layer. When the crack opening increases to a certain point, fracture in the bottom copper starts, and gradually propagates to fracture in the substrate and top copper. Accurate measurement of sensor fracture can be difficult during the experiment. It is likely that a large amount of the observed resonance frequency shift is due to antenna strain/deformation caused by the underlying crack opening, instead of antenna fracture.

The crack size underneath the sensor can also be used to estimate the average strain level experienced by the sensor:

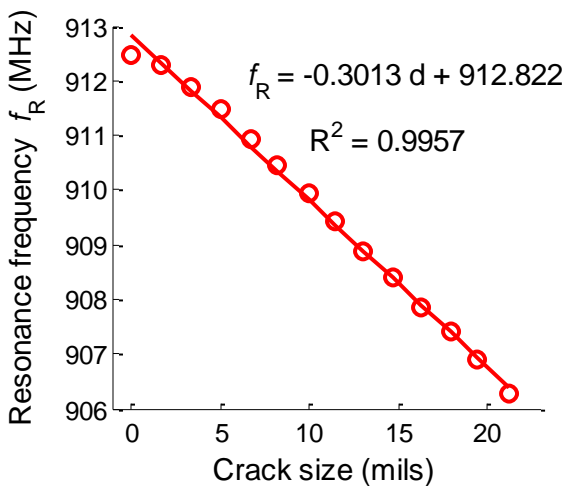


Fig. 10. Relationship between resonance frequency and crack size

$$\varepsilon_{\text{avg}} = \frac{d}{L_T} \quad (4)$$

where  $\varepsilon_{\text{avg}}$  is the average strain of the sensor,  $d$  is the crack size under the sensor, and  $L_T$  is the total length of the sensor ground plane. For each crack opening size, the equivalent strain level is calculated. Relationship between the sensor resonance frequency and the experienced equivalent strain level is shown in Fig. 11. The equivalent strain sensitivity is -0.000723 MHz/ $\mu\varepsilon$ , which means that  $1\mu\varepsilon$  experienced by the sensor generates 723 Hz decrease in resonance frequency. The results matches well with the strain sensitivity previously reported in (Yi *et al.* 2011a), when no strain transfer calibration was performed.

#### 4 SUMMARY AND DISCUSSION

This paper describes the crack sensing performance of a wireless battery-free antenna sensor. The sensor characteristics are first studied by numerical simulation, which illustrates potential resonance frequency change due to a crack. To verify the crack sensing performance, a crack testing device is designed and fabricated. The resonance frequency of the prototype sensor is interrogated by the Tagformance Lite reader at different crack opening sizes. The experimental results show that the antenna sensor is capable of sensing milli-inch crack width and tracking its propagation. The crack sensitivity is reasonable and the equivalent strain sensitivity is consistent with the sensitivity reported in previous studies.

Since electrical current density is not uniform on the entire ground plane of the antenna sensor, different sensitivities can be achieved when the crack occurs at different areas on the ground plane. Moreover, if the crack is not exactly along the width

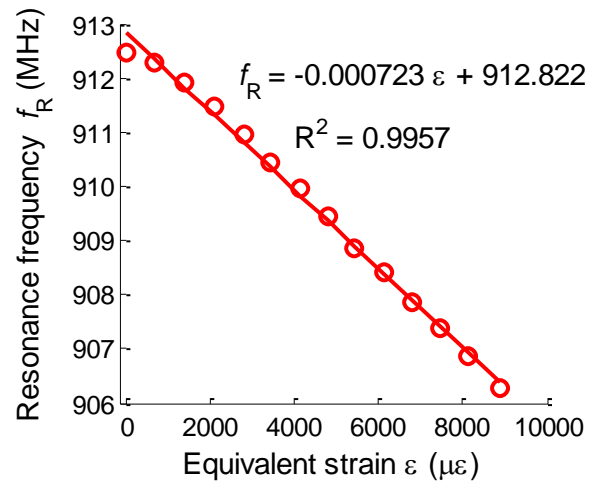


Fig. 11. Relationship between resonance frequency and equivalent strain

direction of the sensor, the crack sensing performance can be different. More experiments are needed to explore the sensing performance under different crack scenarios. Furthermore, multiple-crack sensing is another complicated scenario that requires investigation in the future.

## 5 ACKNOWLEDGEMENT

This material is based upon work supported by the Federal Highway Administration under agreement No. DTFH61-10-H-00004. Any opinions, findings, and conclusions or recommendations expressed in this publication are those of the authors and do not necessarily reflect the view of the Federal Highway Administration.

## 6 REFERENCES

- AASHTO. 2009. *Manual of Bridge Evaluation*, American Association of State Highway & Transportation Officials, Washington D.C.
- ASCE. 2009. *Report Card for America's Infrastructure*, American Society of Civil Engineers: Reston, VA.
- ASNT. 2009. *Nondestructive Testing Handbook*, American Society for Nondestructive Testing, Inc.: Columbus, OH.
- Balanis, C. A. 1997. *Antenna Theory: Analysis and Design*, John Wiley & Sons: New York.
- Dasgupta, A., and Pecht, M. 1991. Material failure mechanisms and damage models. *IEEE Transactions on Reliability* 40(5): 531-536.
- Deshmukh, S., Mohammad, I., Xu, X., and Huang, H. 2010. Unpowered antenna sensor for crack detection and measurement. *Proceeding of SPIE, Sensors and Smart Structures Technologies for Civil, Mechanical, and Aerospace Systems*, 764742.
- Finkenzeller, K. 2003. *RFID Handbook*, John Wiley & Sons: New York.
- Giurgiutiu, V. 2005. Tuned Lamb wave excitation and detection with piezoelectric wafer active sensors for structural health monitoring. *Journal of Intelligent Material Systems and Structures* 16(4): 291-305.
- Ihn, J.-B., and Chang, F.-K. 2004. Detection and monitoring of hidden fatigue crack growth using a built-in piezoelectric sensor/actuator network: I. Diagnostics. *Smart Materials and Structures* 13: 609-620.
- Kurokawa, K. 1965. Power waves and the scattering matrix. *Microwave Theory Technology, IEEE Transactions on* 13(3): 194-202.
- Roberts, T. M., and Talebzadeh, M. 2003. Acoustic emission monitoring of fatigue crack propagation. *Journal of Constructional Steel Research* 59: 695-712.
- Stephens, R. I., Fatemi, A., and Stephens, R. R. 2000. *Metal Fatigue in Engineering*, John Wiley & Sons.
- Yi, X., Wu, T., Wang, Y., Leon, R. T., Tentzeris, M. M., and Lantz, G. 2011a. Passive wireless smart-skin sensor using RFID-based folded patch antennas.

*International Journal of Smart and Nano Materials* 2(1): 22-38.

Yi, X., Wu, T., Lantz, G., Cooper, J., Cho, C., Wang, Y., Tentzeris, M. M., and Leon, R. T. 2011b. Sensing resolution and measurement range of a passive wireless strain sensor. *Proceedings of the 8th International Workshop on Structural Health Monitoring*, Stanford, CA, USA.